Nuclear Charge Radii of $^{78-100}$Sr by Nonoptical Detection in Fast-Beam Laser Spectroscopy

R. E. Silverans, P. Lievens, and L. Vermeeren
Instituut voor Kern- en Stralingsfysika, Leuven University, B-3030 Leuven, Belgium

E. Arnold, W. Neu, R. Neugart, and K. Wendt
Institut für Physik, Universität Mainz, D-6500 Mainz, Federal Republic of Germany

F. Buchinger and E. B. Ramsay
Foster Radiation Laboratory, McGill University, Montreal, Canada H3A 2B2

and

G. Ulm
The ISOLDE Collaboration, CERN, CH-1211 Geneva, Switzerland
(Received 22 January 1988)

We report the application of a new nonoptical detection scheme in laser spectroscopy on ion beams of on-line isotope separators. The method consists of ground-state depopulation by optical pumping in collinear laser–ion-beam interaction, state-selective neutralization, and charge-state–separated fast-atom counting. Strontium isotope-shift measurements are extended into the strongly deformed region of the neutron-rich isotopes up to ^{100}Sr. The radii are generally well described by the droplet model including empirical deformations obtained from $B(E2)$ values.

PACS numbers: 21.10.Ft, 23.20.Qz, 27.50.+e, 27.60.+j

The series of strontium ($Z=38$) isotopes reaches from the valley of stability (at $N=50$) with isotopes showing spherical shape to strongly deformed isotopes within $\Delta N=10$ on both sides of the stability line. The nuclides in this region have found considerable interest from the experimental as well as from the theoretical physics side.[1-4] The predicted strong ground-state deformation at $N\approx 40$ and $N\approx 60$ (Möller and Nix[5]) has been established in a series of nuclear-spectroscopy experiments[6-8] which yield quadrupole deformations of $\beta\approx 0.4$ from the reduced transition probabilities. Ground-state deformations in isotopic series are reflected also in the changes of mean square charge radii $\delta\langle r^2\rangle$ derived from optical isotope-shift measurements.[9] A model-dependent interpretation of the $\delta\langle r^2\rangle$ values has to be carried out and a first approach is commonly done in the frame of a macroscopic model, e.g., the droplet model.[10] In the Sr case, the unique situation of the availability of deformation data from $B(E2)$ values in the regions of strong deformation as well as in the transitional region of the neutron-deficient isotopes allows a stringent test of this approach, provided that the isotope-shift measurements can be extended into both deformation regions far off stability. So far isotope-shift data for $^{78-90}$Sr are available from experiments using optical detection.[11,12]

In this Letter, we report upon extended isotope-shift measurements including the strongly deformed neutron-rich isotopes up to ^{100}Sr. We introduce a new method of nonoptical detection in laser-spectroscopy experiments directly on the fast-ion beams of an on-line isotope separator. The techniques using optical detection are limited by the moderate overall fluorescent photon-counting efficiency and the unavoidable background from scattered laser light.[13] The basic idea behind current experimental developments is to increase the sensitivity in on-line applications by turning to nonoptical detection schemes.[14-19] Our scheme is based on the detection of resonant laser optical pumping by state-selective neutralization and particle counting. This technique is dedicated to measurements on alkaline-earth ions,[19] and it is complementary to the recently developed collisional-ionization technique for rare gases.[18]

The experiments are performed at the ISOLDE on-line isotope separator[20] at CERN. With use of the 600-MeV proton beam of the CERN synchrocyclotron, neutron-rich strontium isotopes are produced by fission reactions in a hot uranium carbide target, whereas the neutron-deficient isotopes are produced by spallation reactions in a niobium-powder target. Fast ion beams, produced by a surface-ionization source, 60-keV acceleration, and mass separation, are deflected to interact collinearly with the light from a cw dye laser, as shown schematically in Fig. 1. The experimental setup allows both classical optical detection and particle detection of the resonant laser-ion interaction. Isotope shifts were investigated in the $5s\,^2S_{1/2}$–$5p\,^2P_{1/2,3/2}$ ($\lambda=421.7$ and 407.9 nm) transitions of Sr II. Classical collinear laser spectroscopy[21] with fluorescent photon detection could be performed for the isotopes ^{78}Sr up to ^{98}Sr. A search on the mass $A=100$ beam gave no indication of an optical-resonance signal. However, the signal of ^{100}Sr was readily observed with the state-selective particle-

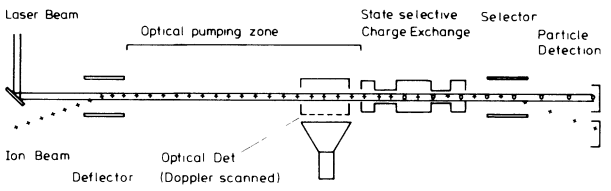

FIG. 1. Schematic experimental setup.

detection scheme (see Fig. 2).

The basic mechanisms of this experimental scheme are the following: At resonance, multiple laser excitation in the optical-pumping zone is followed by deexcitation through $5p\,^2P_J$-$4d\,^2D_{J'}$ and leads to strong population of the low-lying metastable states. This change in the ionic states is efficiently translated into a change in charge state of the beam particles by passage through a Na-vapor charge-exchange cell. The neutralization reaction is strongly state selective through the dependence of the neutralization cross sections on the energy defects for the states involved: $\sigma(4d)/\sigma(5s) \approx 1.5$.[19] The analysis of the charge state of the beam is performed by electrostatic separation of ions and atoms which are counted via the secondary electrons emitted by impact of the particles on an aluminum tape. The isotope shift of ^{100}Sr relative to the lighter isotopes is measured by the alternate use of particle detection (for $A=100$) and optical detection (for two reference isotopes). To have a consistency check with the purely optical-detection measurements, the isotope shift of ^{98}Sr was also measured by particle detection.

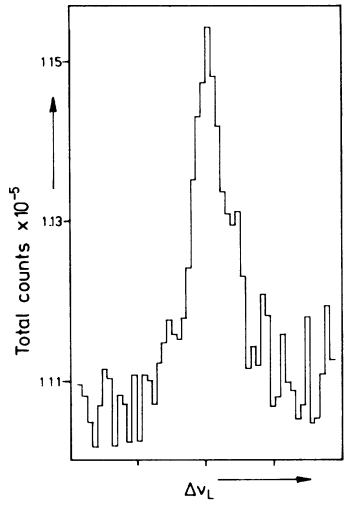

FIG. 2. Particle-detection $^2S_{1/2}$-$^2P_{3/2}$ resonance signal of ^{100}Sr II (2 s/channel laser frequency scan).

Before turning to the interpretation of the present results, we briefly discuss the sensitivity of the new method. The strong resonance signal observed for about 10^4 ions/s of ^{100}Sr is due to the fact that an appreciable fraction of about 10^{-1} of the ions effectively contributes to the resonance signal. With use of isotopically pure strontium beams,[22] the signal-to-background ratio (S/B) equals 0.4, requiring about 10^2 ions/s for an experiment under ideal conditions. Under the present conditions, isobaric contaminants and incomplete optical pumping reduced the S/B by a factor of 10. Still this corresponds

TABLE I. Isotope shifts and changes in mean square charge radii relative to $A=88$ for the even strontium isotopes.

Mass number	Isotope shift (MHz)	$\langle r^2\rangle^A - \langle r^2\rangle^{88}$ (fm^2) This work[a]	Ref. 11[b]	Ref. 12[c]
78	−893(12)	0.242(8)[41]		0.237(9)
80	−782(11)	0.243(7)[33]	0.227(20)	0.249(6)
82	−574(10)	0.179(6)[24]	0.169(13)	0.182(6)
84	−373(5)	0.116(3)[16]	0.110(9)	0.116(4)
86	−171(3)	0.050(2)[8]	0.047(5)	0.046(6)
90	−349(6)	0.277(4)[12]	0.23(9)	
92	−636(8)	0.512(5)[21]		
94	−876(9)	0.715(6)[30]		
96	−1198(10)	0.968(6)[40]		
98	−2155(13) −2166(11)[d]	1.625(6)[59]		
100	−2415(23)[d]	1.832(15)[69]		

[a]Experimental errors with use of the procedure of Ref. 21 are given in parentheses; errors including systematic errors due to uncertainties in the evaluation of $\delta\langle r^2\rangle$ from the isotope shift are given in square brackets.

[b]Data of set 1, King-plot errors included. Data of set 2 are ~30% higher.

[c]Experimental errors only.

[d]Measured with the particle-detection method.

to a required yield of 5×10^2 ions/s. This has to be compared with an optical-detection limit of about 10^5 ions/s due to an overall optical-detection efficiency of 10^{-3} and the high background from laser stray light. The state-selective particle-detection method furthermore offers a supplementary advantage with respect to future experiments on odd isotopes. Measurements on hyperfine-split states are often hampered by hyperfine pumping's reducing the optically detected resonance signal. A two-step ground-state depopulation pumping process cancels the hyperfine pumping and brings the resonance signal intensity of all hyperfine components to the level of the strongest line.[19]

The isotope-shift results for all the investigated even isotopes are presented in Table I. Changes in mean square charge radii were deduced. Contrary to the earlier results on the Sr isotopes with $N \leq 50$, they were obtained in the Sr II transition $5s\,^2S_{1/2}$-$5p\,^2P_{3/2}$ which is considered most reliable for the semiempirical calculation[23] of the electronic factor F. Therefore, we have abandoned the previous analysis based on extensive studies of the Sr I spectrum in combination with muonic-x-ray data[24] and directly calculated $F=-1582(49)$ MHz/fm^2 following the standard procedure and using the latest tabulated values of $C_{\text{unif.}}$.[25] In addition to the normal mass shift S_N, a specific mass shift of $-0.13(11)S_N$ was deduced from a King plot of our data with muonic-isotope shifts.[26] Our $\delta\langle r^2\rangle$ values largely agree with those of Refs. 11 and 12 for the neutron-deficient isotopes (see Table I). For the neutron-rich isotopes, also the symmetry with respect to $N=50$ in the following droplet-model description infers a proper choice of the calibration factor F. For the isotopes listed in Table I the changes of $\langle r^2\rangle$ relative to ^{88}Sr are shown in Fig. 3. A decrease is observed when the neutron-shell closure at $N=50$ is approached from the neutron-deficient side. For higher N, $\langle r^2\rangle$ increases almost linearly except for the dramatic increase between $N=58$ and $N=60$ which corresponds to 2.7 times the average variation found in the preceding and following neutron-rich isotopes.

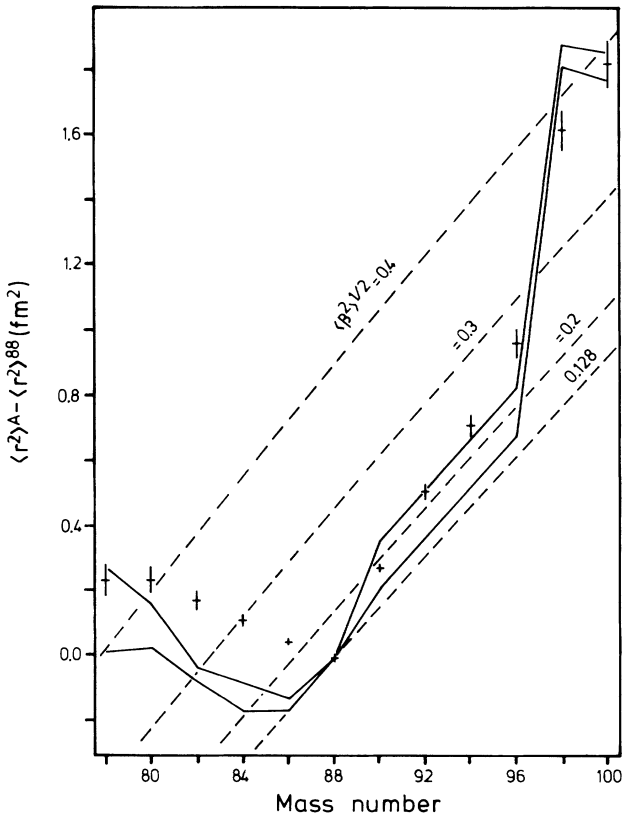

FIG. 3. Experimental changes in mean square charge radii (error bars include systematic errors). Droplet-model isodeformation curves (dashed lines) and a comparison with $\delta\langle r^2\rangle$ calculated from $B(E2)$ values (error bands indicated as solid lines) are added. $\langle\beta^2\rangle^{1/2}=0.128(4)$ for ^{88}Sr was used as the reference.

The variation of the $\langle r^2\rangle$ can be interpreted in the frame of the droplet model[10] by (i) a change of the volume of the charge distribution, (ii) a change of its deformation, and (iii) a change in the central part of the charge distribution due to Coulomb repulsion. If we restrict the deformation part in first order to a change in quadrupole deformation and assume a constant diffuseness parameter, $\delta\langle r^2\rangle$ can be written as

$$\delta\langle r^2\rangle^{(88,A)} = \tfrac{3}{5}R_Z^{2(A)}[1+(5/4\pi)\langle\beta^2\rangle(A)]+\langle r^2\rangle_{\text{red}}^{(A)} - \tfrac{3}{5}R_Z^{2(88)}[1+(5/4\pi)\langle\beta^2\rangle^{(88)}]-\langle r^2\rangle_{\text{red}}^{(88)}, \quad (1)$$

with R_z the proton sharp radius, $\langle\beta^2\rangle$ the mean square quadrupole deformation parameter, and $\langle r^2\rangle_{\text{red}}$ the redistribution term attributed to the respective isotopes. The droplet values for the changes in $\langle r^2\rangle$ were calculated with the model parameters given by Berdichevsky and Tondeur[27] and are included in Fig. 3 as a set of isodeformation lines. From a comparison of these lines with the experimental data it is evident that the observed trend of the radii expresses mainly the change of deformation of the nuclear charge distribution. As expected from nuclear-spectroscopy data, high ground-state deformations of $\langle\beta^2\rangle^{1/2}\approx0.4$ are indicated at the extrema of the isotopic chain at $A\approx78$ and 100. It is also consistent with spectroscopy information that the onset of deformation seems to occur more gradually for the light isotopes, whereas a sudden change from a near spherical to strongly deformed shape is observed for the neutron-rich isotopes between $A=96$ and 98. More quantitatively, the experimental $\delta\langle r^2\rangle$ values can be compared with calculated ones obtained from the droplet model with use of $\langle\beta^2\rangle$ from experimental $B(E2)$ values.[28,29] To be consistent with the droplet-model description of the radii, we used values calculated in the frame of this model,[10,27]

which are only slightly different from the tabulated ones.[28] For those isotopes for which no $B(E2)$ values are available ($90 \leq A \leq 96$), the quadrupole deformation is estimated from the energy of the first excited 2^+ level.[30] The calculated curves are included in Fig. 3. Comparing the experimental $\delta\langle r^2\rangle$ values with the calculated ones, we state good agreement between both sets for neutron-rich isotopes[31] and also for the most strongly deformed isotopes on the neutron-deficient side. Some disagreement is observed only in the transitional region $82 \leq A \leq 88$.

Apart from details the general trends of our present $\delta\langle r^2\rangle$ curve for the Sr isotopes agree rather well with those in the neighboring odd-Z element Rb.[14] The latter has served as a test case for the investigation of the influence of collective zero-point motion on the development of the mean square charge radii.[32] It was concluded by Myers and Rozmej that theoretical values for the collective width $\langle\epsilon^2\rangle$ or $\langle\beta^2\rangle$ fail to explain the sharp change in the slope of the $\delta\langle r^2\rangle$ curve at $N=50$. Reasons for this discrepancy were sought in higher-order multipole contributions or in single-particle core-polarization effects. For the doubly even Sr isotopes, the measured $B(E2)$ values offer empirical information about the $E2$ strength connected with the nuclear ground state.[33] It is obvious from Fig. 3 that the droplet model with these empirical values for $\langle\beta^2\rangle$ gives a substantially better agreement with the experimental data. Therefore, it should be examined to what extent the collective zero-point motion based on a Nilsson single-particle potential reproduces the experimentally observed $E2$ strength.

Possible reasons for the remaining mismatch in the transitional region $82 \leq A \leq 88$ where already discussed for the stable Sr isotopes by Buchinger *et al.*[34] and attributed to changes in the diffuseness of the charge distribution. How far this picture can be extended to the isotopes further off stability will be investigated in a more comprehensive analysis of the experimental data which includes also hfs data now being evaluated.[35] In this respect we expect also a better understanding of the variation of the $\langle r^2\rangle$ in Sr from a combined interpretation of the data in the droplet as well as in a microscopic model.

This work was supported by the Belgian Interuniversity Institute for Nuclear Science (IIKW), the Canadian Natural Sciences and Engineering Research Council, and the German Federal Minister for Research and Technology (BMFT) under Contract No. 06MZ458I. One of us (R.E.S.) is a research associate of the Belgian Foundation for Scientific Research (NFWO).

[1]K. Heyde, J. Moreau, and M. Waroquier, Phys. Rev. C **29**, 1859 (1984).

[2]W. Nazarevitch *et al.*, Nucl. Phys. **A435**, 397 (1985).

[3]K. P. Lieb, L. Lühmann, and B. Wörmann, in *Nuclei Off the Line of Stability,* edited by R. A. Meyer and D. S. Brenner, ACS Symposium Series Vol. 324 (American Chemical Society, Washington, DC, 1986), p. 233.

[4]P. Bonche *et al.*, Nucl. Phys. **A443**, 39 (1985).

[5]P. Möller and J. R. Nix, At. Data Nucl. Data Tables **26**, 165 (1981).

[6]C. J. Lister *et al.*, Phys. Rev. Lett. **49**, 308 (1982).

[7]F. Schussler *et al.*, Nucl. Phys. **A339**, 415 (1980).

[8]R. E. Azuma *et al.*, Phys. Lett. **86B**, 5 (1979).

[9]R. Neugart, in *Lasers in Nuclear Physics,* edited by C. E. Bemis, Jr., and H. K. Carter (Harwood, Chur, 1982), p. 231.

[10]W. D. Myers and K. H. Schmidt, Nucl. Phys. **A410**, 61 (1983).

[11]M. Anselment *et al.*, Z. Phys. A **326**, 493 (1987).

[12]D. A. Eastham *et al.*, Phys. Rev. C **36**, 1583 (1987).

[13]Fluorescent atom coincidence spectroscopy, a method to suppress the background, was demonstrated in Ref. 12.

[14]C. Thibault *et al.*, Phys. Rev. C **23**, 2720 (1981).

[15]V. I. Balykin *et al.*, Usp. Fiz. Nauk **132**, 293 (1980) [Sov. Phys. Usp. **23**, 651 (1980)].

[16]E. Arnold *et al.*, Phys. Lett. B **197**, 311 (1987).

[17]K. Wallmeroth *et al.*, Phys. Rev. Lett. **58**, 1516 (1987).

[18]R. Neugart, W. Klempt, and K. Wendt, Nucl. Instrum. Methods Phys. Res., Sect. B **17**, 354 (1986).

[19]R. E. Silverans, P. Lievens, and L. Vermeeren, Nucl. Instrum. Methods Phys. Res., Sect. B **26**, 591 (1987).

[20]H. L. Ravn, Phys. Rep. **54**, 201 (1979).

[21]A. C. Mueller *et al.*, Nucl. Phys. **A403**, 234 (1983).

[22]S. V. Andreev, V. I. Mishin, and V. S. Letokhov, Opt. Commun. **57**, 317 (1986).

[23]K. Heilig and A. Steudel, At. Data Nucl. Data Tables **14**, 613 (1974).

[24]D. Bender *et al.*, Z. Phys. A **318**, 291 (1984).

[25]S. A. Blundell *et al.*, Z. Phys. A **321**, 31 (1985).

[26]R. Engfer *et al.*, At. Data Nucl. Data Tables **14**, 509 (1974).

[27]D. Berdichevsky and F. Tondeur, Z. Phys. A **322**, 141 (1985).

[28]S. Raman, At. Data Nucl. Data Tables **36**, 1 (1987), and references therein.

[29]H. Ohm *et al.*, Z. Phys. A **327**, 483 (1987).

[30]L. Grodzins, Phys. Lett. **2**, 88 (1962).

[31]The decrease in deformation from ^{98}Sr to ^{100}Sr recently reported in Ref. 29 is not confirmed by our results.

[32]W. D. Myers and P. Rozmej, Nucl. Phys. **A470**, 107 (1987).

[33]K. Kumar, Phys. Rev. Lett. **28**, 249 (1972).

[34]F. Buchinger *et al.*, Phys. Rev. C **32**, 2058 (1985).

[35]Spin assignments have been reported by F. Buchinger *et al.*, Z. Phys. A **327**, 361 (1987).